Cone-beam Tomography from Short-Scan Circle-plus-Arc Data Measured on a C-arm System

Stefan Hoppe, *Student Member, IEEE,* Frank Dennerlein, *Student Member, IEEE,*
Günter Lauritsch, Joachim Hornegger, and Frédéric Noo, *Member, IEEE*

***Abstract*— In C-arm computed tomography (CT) systems, the source trajectory does not follow an ideal trajectory. Thus, the real data acquisition geometry is typically expressed by a sequence of projection matrices. However, exact reconstruction algorithms are based on an analytic expression of the projection geometry. In this work, we present a reformulation of an exact reconstruction method to handle projection matrices. In particular, the M-line approach is investigated for a short-scan circle-plus-arc data acquisition. The computation of the derivative with respect to the source trajectory is numerically most critical for which a novel and stable implementation is developed. In order to determine the backprojection range, a 2D polygonal weighting scheme is proposed. Image results are presented from phantom data acquired by a Siemens AXIOM Artis C-arm system. Excellent image results are achieved. Due to the complete data acquisition, the problem of cone artifacts is totally resolved.**

I. Introduction

On C-arm systems, the data acquisition geometry is usually described by a set of projection matrices rather than by analytical equations, because C-arm systems are not able to acquire data along an ideal source trajectory [1]. For approximate reconstruction approaches like the FDK algorithm [2], these deviations are only taken into account in the backprojection step (see also [3]). However, when exact image reconstruction is applied, deviations from an ideal description of the acquisition geometry have to be considered carefully in each processing step (including the filtering step) in order to ensure the accuracy of the approach. In this work, formulae are presented to adapt the algorithmic steps of an exact filtered backprojection (FBP) algorithm recently proposed in [4] (denoted as M-line algorithm in the following) to process information provided by a sequence of projection matrices. The proposed algorithm is able to process cone-beam (CB) data measured on a real C-arm system. A novel and numerically stable implementation was developed to compute the derivative with respect to the source trajectory. In order to determine the backprojection range, a 2D polygonal weighting scheme is proposed. The system was configured to collect data on a circle-plus-arc source trajectory. This trajectory is complete according to Tuy's sufficiency theorem [5] and can easily be performed with C-arm systems. The M-line algorithm can easily be applied to real trajectories because it does not assume an ideal description of the acquisition geometry. Alternative reconstruction algorithms as e.g. [6] for the circle-plus-arc geometry are available but require a different adaptation to deal with real data (see [7] for a recently proposed scheme). Real data is acquired with an AXIOM Artis *d*BA C-arm system (Siemens AG, Medical Solutions, Forchheim, Germany). Reconstruction results of the adapted M-line algorithm using a complete trajectory are compared to a state-of-the-art FDK algorithm using a short-scan circular path only.

S. Hoppe and J. Hornegger are with the Institute of Pattern Recognition (LME), University of Erlangen-Nuremberg, Erlangen, Germany.

F. Noo and F. Dennerlein are with the Department of Radiology (UCAIR), University of Utah, Salt Lake City, UT, USA.

G. Lauritsch is with the Siemens AG, Medical Solutions, Forchheim, Germany.

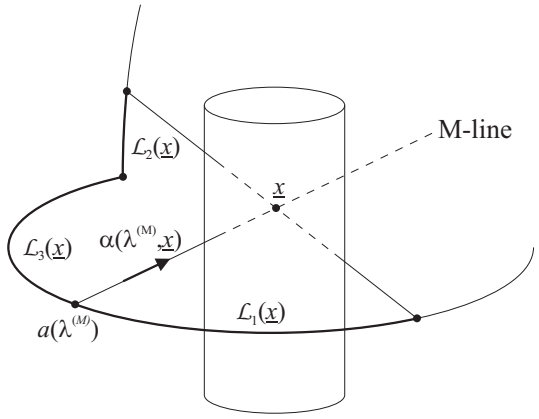

Fig. 1. For each reconstruction point $\underline{x}$, backprojection is performed over three segments $\mathcal{L}_1(\underline{x}), \mathcal{L}_2(\underline{x}), \mathcal{L}_3(\underline{x})$ and then the contributions are accumulated [4].

II. Theoretical Background

The task in image reconstruction is to recover the density of an object $f(\underline{x})$ under examination provided a set of line integrals

$$g(\lambda, \underline{\theta}) = \int_0^\infty f(\underline{a}(\lambda) + t\underline{\theta})dt, \tag{1}$$

where λ denotes the source trajectory parameter, $\underline{a}(\lambda)$ describes the corresponding source position and $\underline{\theta}$ the direction of the line. If we assume a flat panel detector located at a distance D from the current source position, each detector value at

coordinates $(u,v)^T$ refers to a line integral with line direction

$$\underline{\theta} = (u\underline{e}_u + v\underline{e}_v - D\underline{e}_w)\,/\sqrt{u^2+v^2+D^2}. \qquad (2)$$

Here, the detector coordinates are identified by two unit normal vectors $\underline{e}_u$ and $\underline{e}_v$ and the coordinate origin $(u_0,v_0)^T = (0,0)^T$ is the orthogonal projection of $\underline{a}(\lambda)$ onto the detector (referred to as the "principal point" in the following). The vector $\underline{e}_w = \underline{e}_u \times \underline{e}_v$ points from the detector towards the source position. In order to apply these equations, all quantities (e.g. $\underline{e}_u, \underline{e}_v, \underline{e}_w, D$) have to be extracted from projection matrices in practice (Section III).

Accurate image reconstruction for a point $\underline{x}$ inside the support of the object can be achieved in three successive steps:

(i) A derivative of the cone-beam data (1) with respect to λ along constant viewing direction $\underline{\theta}$ has to be computed which is regarded here as the following limit

$$g'(\lambda,\underline{\theta}) = \lim_{\epsilon\to 0} \frac{g(\lambda+\epsilon,\underline{\theta}) - g(\lambda-\epsilon,\underline{\theta})}{2\epsilon}. \qquad (3)$$

The computation of this derivative involves a preprocessing of the detector content as well as an interpolation between neighboring projections on the source trajectory (Section IV).

(ii) A one-dimensional filtering operation has to be applied to the derivative of the cone-beam data along the projection of a so called "M-line" with direction $\underline{\alpha}(\lambda^{(M)},\underline{x})$, which connects the point $\underline{a}(\lambda^{(M)})$ on the source trajectory to the point $\underline{x}$ where reconstruction has to be achieved (Section V).

(iii) The filtered result has to be backprojected into the image space. Backprojection is carried out over three segments $\mathcal{L}_1(\underline{x}), \mathcal{L}_2(\underline{x}), \mathcal{L}_3(\underline{x})$ which depend on the specific point $\underline{x}$ and its M-line (Figure 1). The union of all three segments constitutes the backprojection interval for the point under consideration (Section VI).

III. Geometry Description using Projection Matrices

The calibration procedure of a C-arm system usually outputs geometry information in the form of projection matrices – one matrix for every source position along the trajectory [1], [3]. The 3×4 projection matrix P defines a mapping of the point $\underline{x}$ onto the detector plane for each source position $\underline{a}(\lambda)$ according to

$$c\cdot(\tilde{u},\tilde{v},1)^T = P\cdot(\underline{x}^T,1)^T, \qquad (4)$$

where c is a homogenous scaling factor. The point $(\tilde{u},\tilde{v})^T$ is defined with respect to the lower left image corner with its units expressed in pixel. In this coordinate system, the principal point has coordinates $(\tilde{u}_0,\tilde{v}_0)^T$. In order to apply the given equations, the point must be transformed using

$$u = (\tilde{u}-\tilde{u}_0)\cdot du \quad \text{and} \quad v = (\tilde{v}-\tilde{v}_0)\cdot dv, \qquad (5)$$

where du and dv denote the pixel width and height respectively. All parameters are obtained by a decomposition of the projection matrix P as follows (see [8] for details):

$$P = \begin{bmatrix} \frac{D}{du} & 0 & \tilde{u}_0 \\ 0 & \frac{D}{dv} & \tilde{v}_0 \\ 0 & 0 & 1 \end{bmatrix} \begin{bmatrix} R & -R\cdot\underline{a}(\lambda) \end{bmatrix}, \qquad (6)$$

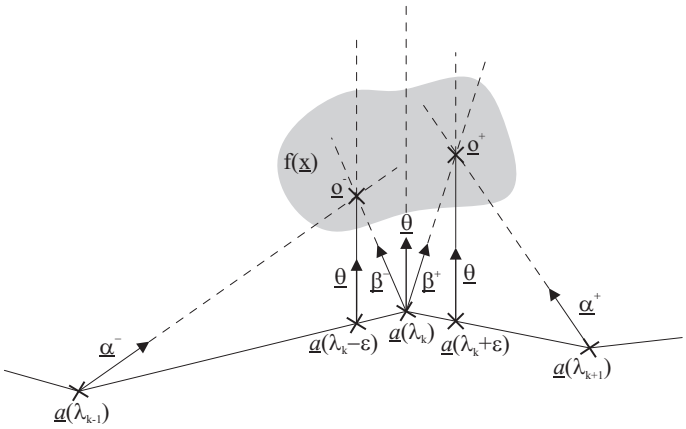

Fig. 2. The proposed interpolation scheme to compute the derivative $g'(\lambda_k,\underline{\theta})$. The trajectory is assumed to be of polygonal shape.

where by definition

$$R = \begin{bmatrix} \underline{e}_u & \underline{e}_v & -\underline{e}_w \end{bmatrix}^T \qquad (7)$$

is a 3×3 matrix which defines the detector orientation.

IV. Computation of the Derivative

In this work, the derivative of the CB data with respect to λ_k along constant viewing direction $\underline{\theta}$ is computed directly using a discrete version of formula (3)

$$g'(\lambda_k,\underline{\theta}) = \frac{g(\lambda_k+\epsilon,\underline{\theta}) - g(\lambda_k-\epsilon,\underline{\theta})}{2\epsilon}, \qquad (8)$$

where $\epsilon\in\mathbb{R}$ is a tuning parameter. Provided that the trajectory is equidistantly sampled at increments $\Delta\lambda$, setting $\epsilon = \Delta\lambda$ amounts to a computation of the derivative involving the CB data $g(\lambda_{k+1},\underline{\theta})$ and $g(\lambda_{k-1},\underline{\theta})$. Due to the low sampling rate along the source trajectory however, ϵ should be chosen such that $\epsilon \ll \Delta\lambda$. Therefore, in our new approach, the CB data $g(\lambda_k \pm \epsilon,\underline{\theta})$ is interpolated from $g(\lambda_k,\underline{\theta})$ and $g(\lambda_{k\pm1},\underline{\theta})$. Generally, we have to find rays with directions $\underline{\alpha}^{\pm}$ and $\underline{\beta}^{\pm}$, such that

$$g(\lambda_k+\epsilon,\underline{\theta}) = \quad g(\lambda_{k+1},\underline{\alpha}^+)\cdot\eta^+ + g(\lambda_k,\underline{\beta}^+)\cdot(1-\eta^+) \qquad (9)$$

$$g(\lambda_k-\epsilon,\underline{\theta}) = \quad g(\lambda_{k-1},\underline{\alpha}^-)\cdot\eta^- + g(\lambda_k,\underline{\beta}^-)\cdot(1-\eta^-), \qquad (10)$$

where

$$\eta^{\pm} = \frac{\|\underline{a}(\lambda_k\pm\epsilon) - \underline{a}(\lambda_k)\|}{\|\underline{a}(\lambda_{k\pm1}) - \underline{a}(\lambda_k)\|} \quad \text{and} \quad \eta^{\pm}\in]0;1]. \qquad (11)$$

The ray directions $\underline{\alpha}^{\pm}$ and $\underline{\beta}^{\pm}$ can be computed according to

$$\underline{\alpha}^{\pm} = \frac{\underline{o}^{\pm} - \underline{a}(\lambda_{k\pm1})}{\|\underline{o}^{\pm} - \underline{a}(\lambda_{k\pm1})\|} \quad \text{and} \quad \underline{\beta}^{\pm} = \frac{\underline{o}^{\pm} - \underline{a}(\lambda_k)}{\|\underline{o}^{\pm} - \underline{a}(\lambda_k)\|}, \qquad (12)$$

where the points $\underline{o}^{\pm}$ are orthogonal projections of the object center onto the lines $\{\underline{x}\in\mathbb{R}^3 | \underline{x} = \underline{a}(\lambda_k\pm\epsilon) + t\underline{\theta}\}$ (Figure 2). In our experiments, ϵ was chosen such that $\|\underline{a}(\lambda_k\pm\epsilon) - \underline{a}(\lambda_k)\| = du = dv$ for a detector with square detector elements.

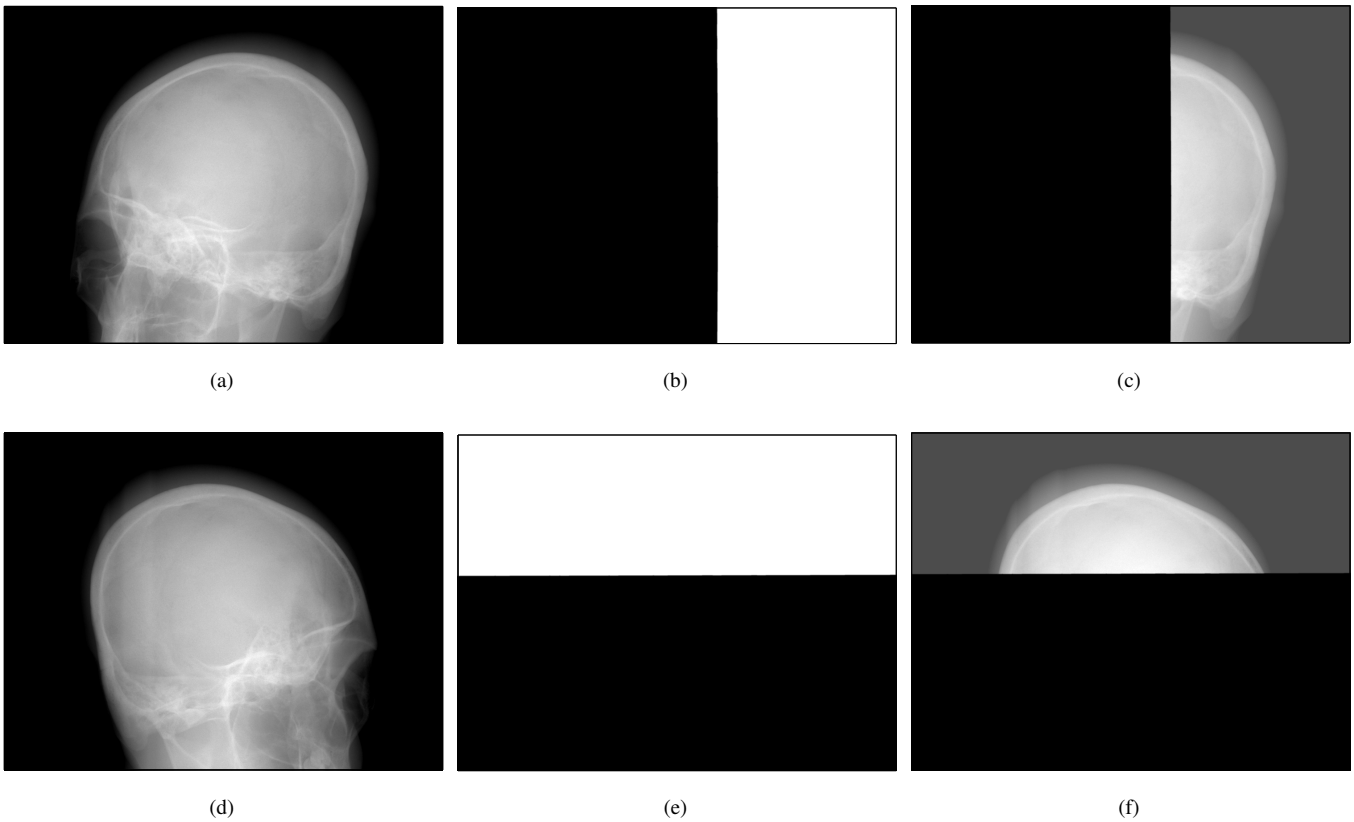

Fig. 3. The backprojection interval is determined by multiplying the projection image (a),(d) with the 2D detector weighting mask (b),(e). The result (c),(f) is backprojected into the image space. The example involves CB data of a human head phantom which was acquired from a source position on segment $\mathcal{L}_1(\underline{x})$ (top) and on segment $\mathcal{L}_2(\underline{x})$ (bottom). For visualization purposes, the unfiltered CB data is displayed.

V. Selection of $\lambda^{(M)}$

As shown in [4], the point $\underline{a}(\lambda^{(M)})$ can be chosen arbitrarily on the source trajectory and may vary for each point $\underline{x}$. However, if all points which have to be reconstructed share the same $\lambda^{(M)}$, the algorithm is of FBP-type and can therefore be implemented efficiently. In this work, $\underline{a}(\lambda^{(M)})$ was chosen to be a source position approximately in the middle of the short-scan, because then the filtering lines have minimal slopes and the long object problem is solved (see Figure 1).

VI. Determination of the Backprojection Interval

The backprojection interval for each point $\underline{x}$ is determined by its R-line (see [4]) which connects two source positions on the trajectory. Backprojection is restricted to the backprojection interval to mask out redundant measurements for that point.

The decision if the current projection at $\underline{a}(\lambda_k)$ is located inside the backprojection interval for a point $\underline{x}$ can be made by projecting a part of the trajectory onto the detector plane and by using only those detector data at the appropriate side of the projected trajectory as shown in [6]. Referring to Figure 1, we project the arc part onto the detector when the source moves along $\mathcal{L}_1(\underline{x})$ or $\mathcal{L}_3(\underline{x})$ and the circle part when the source moves along $\mathcal{L}_2(\underline{x})$. Because an analytical description of the trajectory is not available, the projections of successive source positions are connected by lines in the detector plane, resulting in a 2D curve of polygonal shape. The polygon is then used to create a 2D detector weighting mask which defines the backprojection region. Within the weighting mask, each pixel outside the backprojection region is assigned a value of zero, each pixel inside is assigned a value of one. Pixels within a small neighborhood to the polygon are assigned a value between zero and one. Thus, a smooth transition zone is generated in order to avoid reconstruction artifacts. The weighting mask needs to be multiplied with the detector content after the filtering step and prior to backprojection (see Figure 3).

VII. Results

We present reconstruction results using complete cone-beam data acquired with an AXIOM Artis *d*BA C-arm system (Siemens AG, Medical Solutions, Forchheim, Germany). Reconstructions are compared to a state-of-the-art FDK implementation. For the M-line approach, a two-sided circle-plus-arc trajectory was used. Depending whether the volume had to be reconstructed below or above the circle plane, one of the two arc contributions was chosen. The circle-plus-arc trajectory was calibrated with the approach described in [9].

Table I shows the parameters used throughout the experiments. Although the sample rate was the same for both algo-

	M-line	FDK
Trajectory	short-scan-plus-arc	short-scan
Radius [mm]	750	750
Focal length (D) [mm]	1200	1200
Pixel width (du) [mm/px]	0.308	0.308
Pixel height (dv) [mm/px]	0.308	0.308
Detector dimension [px^2]	1240 × 960	1240 × 960
Angular sampling (circle) [°/projection]	0.4	0.4
Angular sampling (arc) [°/projection]	0.4	—
Number of projections (circle)	644 (257.2°)	644 (257.2°)
Number of projections (arc)	53 (20.8°)	—
Isotropic voxel length [mm]	0.25	0.25

TABLE I

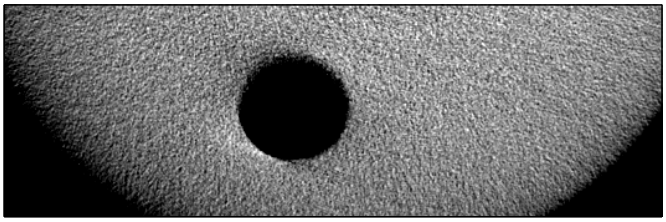

(a)

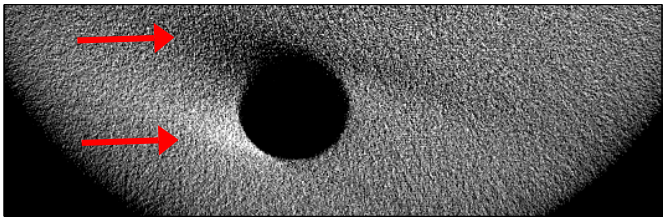

(b)

Fig. 4. Reconstruction of the cone-beam phantom with disc shaped inlays for (a) the M-line algorithm and (b) the FDK algorithm. The slices are 43 mm away from the plane of the short-scan. The window was set to C=0 HU, W=600 HU.

rithms, the M-line approach in addition needs 53 projections for the arc segment (which was also sampled with an angular increment of 0.4°).

In Figure 4 and Figure 5, reconstructions of a cone-beam phantom with inlays of varying shape and density are shown. The slices are close to the z-edges of the inlays. The M-line reconstruction result is free of cone artifacts which appear in the FDK reconstruction as black and white shadows in the vicinity of the inlays. The different appearance of the left wedge in Figure 5a compared to Figure 5b might be caused by a different slice sensitive profile of M-line versus FDK which has to be investigated in the future.

In Figure 6, one slice of a human head phantom which was reconstructed with the M-line approach is shown. Again, the result is free of cone artifacts and even small details can be distinguished.

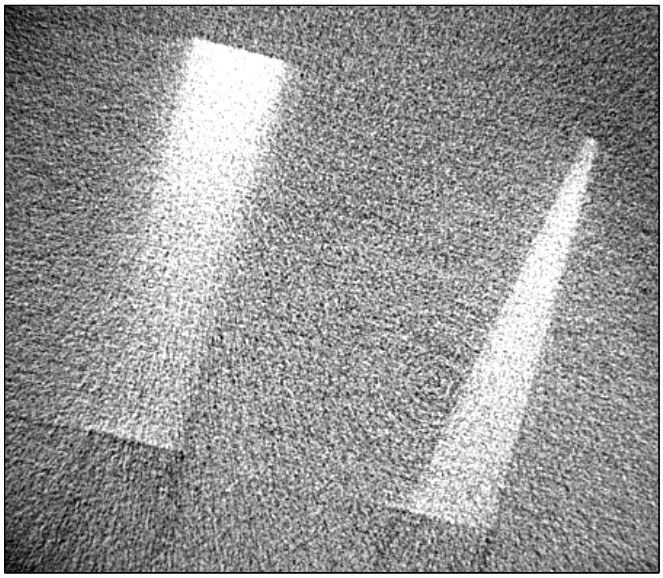

(a)

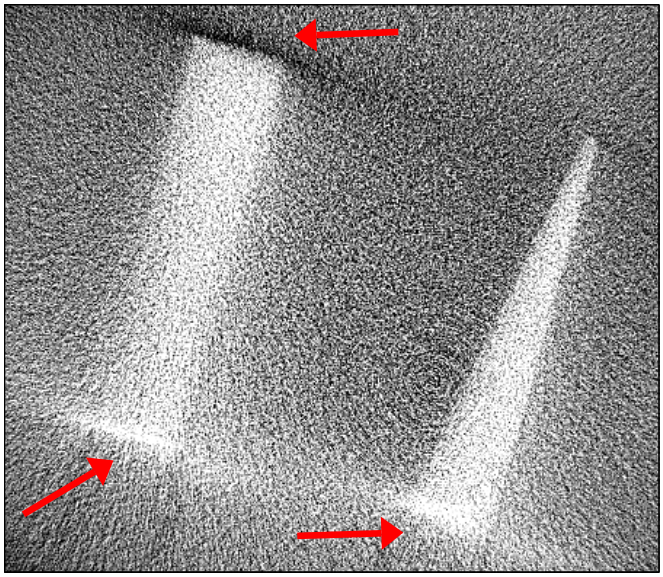

(b)

Fig. 5. Reconstruction of the cone-beam phantom with wedge shaped inlays for (a) the M-line algorithm and (b) the FDK algorithm. The slices are 77 mm away from the plane of the short-scan. The window was set to C=0 HU, W=600 HU.

VIII. Conclusions

We have shown how to adapt the main algorithmic steps of the M-line algorithm to deal with a sequence of projection matrices. Reconstruction results using a real data acquisition setting were presented. Our experiments have shown that the M-line algorithm provides excellent image quality. Since a short-scan circle-plus-arc trajectory provides complete data, the problem of cone artifacts is totally resolved. The proposed

Fig. 6. Reconstruction of the human head phantom for the M-line algorithm. The slice is 27 mm away from the plane of the short-scan. The window was set to C=0 HU, W=600 HU.

method is easily adaptable to other source trajectories in the context of the M-line algorithm.

ACKNOWLEDGMENTS

This work was supported by Siemens AG, Medical Solutions and was supported in part by the U.S. National Institutes of Health (NIH) under grant R01 EB000627.

REFERENCES

[1] N. Strobel, B. Heigl, T. Brunner, O. Schuetz, M. Mitschke, K. Wiesent, and T. Mertelmeier. Improving 3d image quality of x-ray c-arm imaging systems by using properly designed pose determination systems for calibrating the projection geometry. *Medical Imaging 2003: Physics of Medical Imaging*, 5030:943–954, 2003.

[2] L.A. Feldkamp, L.C. Davis, and J.W. Kress. Practical cone-beam algorithm. *J. Opt. Soc. Am. A*, 1(6):612–619, 1984.

[3] K. Wiesent, K. Barth, N. Navab, P. Durlak, T. Brunner, O. Schuetz, and W. Seissler. Enhanced 3-d-reconstruction algorithm for c-arm systems suitable for interventional procedures. *IEEE Transactions on Medical Imaging*, 19(5):391–403, 2000.

[4] J. Pack and F. Noo. Cone–beam reconstruction using 1d filtering along the projection of m–lines. *Inverse Problems*, 21(3):1105–1120, 2005.

[5] H.K. Tuy. An inversion formula for cone–beam reconstruction. *SIAM J. Appl. Math.*, 43(3):546–552, 1983.

[6] A. Katsevich. Image reconstruction for the circle–and–arc trajectory. *Physics in Medicine and Biology*, 50(10):2249–2265, 2005.

[7] F. Dennerlein, A. Katsevich, G. Lauritsch, and J. Hornegger. Exact and efficient cone-beam reconstruction algorithm for a short-scan circle combined with various lines. *Proc. of SPIE*, 5747:388–399, 2005.

[8] R. Hartley and A. Zisserman. *Multiple View Geometry in Computer Vision*. Cambridge University Press, 2nd edition, March 25, 2003.

[9] S. Hoppe, F. Noo, F. Dennerlein, G. Lauritsch, and J. Hornegger. Calibration of the circle-plus-arc trajectory. In *IEEE Medical Imaging Conference*, San Diego, CA, USA, Oct. 29 - Nov. 4, 2006 (to appear).